

Polymer-bound osmium oxide catalysts ¹

Wolfgang A. Herrmann ^{a,*}, Roland M. Kratzer ^a, Janet Blümel ^a,
Holger B. Friedrich ^b, Richard W. Fischer ^c, David C. Apperley ^d, Janos Mink ^{e,f},
Otto Berkesi ^e

^a Anorganisch-chemisches Institut, Technische Universität München, D-85747 Garching bei München, Germany

^b Department of Chemistry, University of Natal, Durban 4041 South Africa

^c Hoechst AG, Central Research, C 487, D-65926 Frankfurt Germany

^d University of Durham, Industrial Research Laboratories, South Road, Durham, DH1 3LE UK

^e Department of Analytical Chemistry, University of Veszprem, Egyetem u. 10, P.O. Box 158, H-8201 Veszprem Hungary

^f Institute of Isotopes of the Hungarian Academy of Science, P.O. Box 77, H-1526 Budapest Hungary

Received 24 June 1996; accepted 1 October 1996

Abstract

Polymer-supported oxidic osmium catalysts based on cross-linked poly(4-vinyl pyridine) were synthesized by various routes and characterized by a number of physical techniques (Raman, IR, XPS, ¹³C and ¹⁵N solid-state NMR spectroscopy). Model compounds of type Os₂O₆L₄ (L = pyridine, 4-*iso*-propyl pyridine, and 4-*tert*-butyl pyridine) were obtained under the conditions of the catalyst synthesis. The catalytic systems were successful in the dihydroxylation of alkenes.

Keywords: Dihydroxylation; Alkenes; Supported catalyst; Osmium

1. Introduction

Although osmium tetroxide is known to catalyze the dihydroxylation of alkenes since the fundamental work of Hofmann, Milas, and Criegee, and in spite of the fact that a well-established enantioselective variant is now available, fruitful industrial applications have never been seen [1–4]. Because of its special biological and physical properties (high toxicity and volatility), the handling of osmium tetrox-

ide is difficult, especially concerning industrial use. Grafting of osmium tetroxide on a suitable support seems to be a way to come closer towards technical applications. In this context, Cainelli et al. reported the preparation of polymersupported catalysts: OsO₄ is immobilized on several amine-type polymers [5]. Such catalysts **1** evidently have structures of the type OsO₄ · L, with the N-group of the polymer (= L) being coordinated to the Lewis acidic osmium center (Fig. 1). Molecular structures of this formula are the monomeric complexes OsO₄ · NR₃ (R = alkyl group) [6]. Based upon this concept, a catalytic enantioselective dihydroxylation was established by using polymers containing cinchona alkaloid derivatives [7].

Independently, we reported the immobiliza-

* Corresponding author. Tel.: +49-89-28913080; fax: +49-89-28913473.

¹ Dedicated to the late Professor Hidemasa Takaya, † October 4, 1996 in Kreuth/Bavaria.

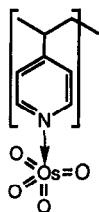


Fig. 1. Structure of catalyst 1.

tion of OsO_4 by stirring OsO_4 with polymers such as poly(4-vinyl pyridine) in THF for a number of days [8]. In the present contribution, we present evidence for the structure of these systems and report on the catalytic properties in the dihydroxylation of alkenes.

2. Results and discussion

In sharp contrast to the Cainelli catalyst 1 (Fig. 1), our loaded polymer **2a** does not contain osmium(VIII)oxide, but oxidic osmium in a lower oxidation state. Thus, during the formation of the catalyst **2a**, the solvent THF serves as a reducing agent. Whilst the Cainelli catalyst 1 does not react with H_2O_2 (8% in *tert*-butanol), **2a** yields the catalyst **2b** (Scheme 1). The resulting catalytic system **2b** shows better and more reproducible results in the dihydroxylation of alkenes than **2a**.

The Cainelli catalyst 1 decomposes over months when stored in air (color change from yellow to black). As shown by TG-MS data, it eliminates OsO_4 already at *room temperature* and *ambient pressure*. Catalysts **2a** and **2b** do not show any change and do not release OsO_4 even upon prolonged storage. Moreover, no loss of OsO_4 is observed in the mass spectrum of catalyst **2b** up to 350°C .

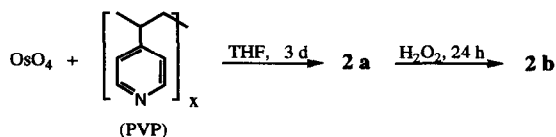
Scheme 1. Synthesis of polymer-bound osmium oxide catalysts **2a** and **2b**.

Table 1

XPS-results of support material and **2a** (BE = binding energy)

Signals	PVP		2a	
	BE (eV)	(at%)	BE (eV)	(at%)
C ₀	—	—	284.4	6.6
C ₁	285.0	23.4	285.0	15.1
C ₂	285.5	38.1	285.5	40.0
C ₃	286.0	25.2	286.1	18.0
C ₄	—	—	286.4	8.3
C ₅	287.3	0.3	—	—
N ₁	399.4	10.7	399.4	8.2
N ₂	—	—	400.8	1.6
Os ₁	—	—	52.6	0.20
Os ₂	—	—	54.5	1.1
Os ₃	—	—	55.1	0.94

According to the results of various analytical methods and in agreement with the structure of model compounds it is likely that an osmium(VI)oxide is formed during the fixation of osmium tetroxide on cross-linked poly(4-vinyl pyridine) (PVP). Even after oxidative treatment (H_2O_2), the osmium species of the resulting catalyst **2b** shows no change in oxidation state. An unequivocal structural assignment was not possible but the following techniques revealed at least general features.

2.1. X-ray photoelectron spectroscopy (XPS)

This method was administered to possibly determine the oxidation state of osmium present on cross-linked PVP after treatment with osmium tetroxide in THF (**2a**) and after the oxidative treatment (**2b**), respectively. Some of the results are shown in Tables 1–3.

A single Os compound with an electron binding energy of ca. 55 eV (4f electrons) dominates the spectrum, quite characteristic for *hexavalent* osmium (e.g., $\text{K}_2[\text{OsO}_2(\text{OH})_4]$, 55.2 eV [9]). In some samples two compounds with similar binding energies (54.8 eV and 55.2 eV) were observed, possibly due to the formation of two different forms of osmium(VI)oxide, e.g. monomeric and dimeric species. This is in line with the electron binding energies of dimeric dioxosmium(VI)complexes: the energies of

Table 2
XPS-results of catalyst **2b** (BE = binding energy)

Signals	PVP/4.5% Os		PVP/5.1% Os	
	BE (eV)	(at%)	BE (eV)	(at%)
C ₀	283.5	1.5	284.5	8.4
C ₁	284.9	11.6	285.0	13.6
C ₂	285.4	37.3	285.5	38.2
C ₃	285.9	17.2	286.0	18.0
C ₄	286.7	7.2	286.5	5.4
			286.9	2.6
C ₅	288.1	3.3	288.3	2.6
N ₁	399.4	6.1	399.5	9.4
N ₂	400.7	1.9	401.0	1.0
Os ₁	52.9	0.08	52.8	0.08
Os ₂	54.9	0.27	54.8	0.27
Os ₃	—	—	55.2	0.28

dinuclear systems are at about 54.3 eV and therefore up to 1 eV lower as compared to the corresponding *mononuclear* compounds [10]. However, an additional minor Os compound (53 eV) is present all the time; it seems to be osmium(IV)oxide OsO₂ (52.7 eV [11]).

The XPS data of catalyst **2b** with additional carbon atom signals at ca. 288 eV (Table 2) indicate the presence of *carboxy* groups in the polymer. Refluxing of **2a** in H₂O₂/*tert*-butanol dissolves the catalyst completely under decomposition. On heating the starting material PVP under the same conditions none of these observations are made. Thus oxidative treatment in the presence of Os seems to partially degrade the polymer, primarily the CC-backbone. The XPS data are in line with this (Table 3): catalyst **2b** exhibits a relative decrease in the backbone signals C₁, whereas the relations of the C₂-,

C₃-, and total N-signals remain roughly unchanged.

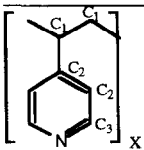
The second nitrogen signal at ca. 401 eV cannot unambiguously be assigned to an Os–N bond because of the changing Os/N ratio. An authentic sample of poly(4-vinyl pyridine-*N*-oxide) shows a binding energy of 403.3 eV. Therefore, due to the lack of signals in this region, the formation of PVP-*N*-oxide [8] can be ruled out, even in case of oxidative treatment.

2.2. CP / MAS NMR spectroscopy

The ¹³C CP/MAS spectra of the PVP support are similar to the data of a material obtained by treatment of PVP with OsO₄ in cyclohexane (**1**, Fig. 2). When the loading is performed in THF (**2a**), usually signals of merely adsorbed THF show up at 26.1 and 68.3 ppm. Both the narrow lines and the solid-state NMR characteristics are indicative of adsorption and not of chemical bonding [12]. Additionally, the intensity of the THF signals decreases upon prolonged drying of the material in a vacuum.

The aliphatic polymer backbone is easily identified by the chemical shifts. There are two overlapping signals (shoulder of the signal at 41 ppm, Fig. 2). The pyridine rings gave signals at 123 and 151 ppm, with intense first-order rotational side-bands due to large chemical shift anisotropes [13,14] in the conventional ¹³C CP/MAS spectrum. When a dipolar dephasing delay of 40 μs was applied, the signals at 41,

Table 3
Ratio of the signals of the support material PVP, PVP stirred in THF, PVP stirred in 8% H₂O₂ in *tert*-butanol and **2b** (mean value)

Polymer	Atom	PVP	PVP/THF	PVP/H ₂ O ₂	2b
	C ₁	2	2	2	2
	C ₂	3.3	3.3	3.3	5.7
	C ₃	2.1	2.1	2.1	2.8
	C ₄	0.02	0.01	0.19	1.1
	N	0.9	0.8	0.7	1.4

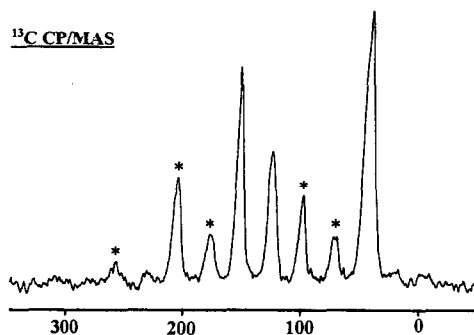


Fig. 2. 75.5 MHz ^{13}C CP/MAS spectrum of poly(4-vinyl pyridine) (PVP) treated with OsO_4 in cyclohexane. The asterisks denote rotational sidebands. Spinning frequency: 4000 Hz.

123, and 151 ppm were substantially reduced in intensity, while a resonance at 154 ppm remains (which had previously been hidden under the broad signal at 151 ppm). On the basis of this experiment, the signal at 154 ppm is assigned to the quaternary carbon atom of the pyridine ring. This is further supported by an increment calculation in analogy to substituted benzenes [15]. For example, *para* substitution of pyridine with an isopropyl group should lead to a ca. 20 ppm downfield shift of the *para* carbon (C_γ) resonance. The observed signal at 154 ppm is in accord with the calculation (156 ppm). The same agreement is found for the non-quaternary C_α (151 ppm) and C_β (123 ppm) resonances.

The ^{13}C CP/MAS spectra do not change after treatment with OsO_4 , showing that the latter does *not* bind to the carbon atoms of the pyridine rings. Binding of OsO_4 via the nitrogen seems at first glance more likely. As is seen from various examples of pyridinium compounds [16], however, the signals of the ring carbon atoms should be shifted substantially to lower frequencies. We therefore conclude that the coverage with OsO_4 (ca. 5%) is too low in order to provide signals other than those of the support. However, ^{13}C CP/MAS NMR can be successfully used in order to study the fate of the catalyst **2a** under the applied conditions. While the support PVP does not change upon treatment with H_2O_2 /*tert*-BuOH after being

loaded with OsO_4 , the support PVP is attacked by this oxidative mixture. The ^{13}C CP/MAS spectrum of **2b** displays a number of signals in the region 150–177 ppm (besides the strong resonance at 41 ppm), the most intense signals occurring at $\delta = 166$ and 177 ppm; these two signals are typical of carboxy groups. The quaternary nature of the corresponding carbons is supported by dipolar dephasing experiments. Hence we conclude in accordance with the aforesaid, that the immobilized catalyst **2a** oxidizes not only the substrate but also the support material. Upon oxidative treatment, most of the oxidation-sensitive sites of the polymer are being oxidized. If catalyst **2b** is used, this 'side reaction' is obviously reduced, resulting in a more reproducible catalytic activity. Moreover, partial cleavage of the polymer backbone could enlarge the numbers of active Os-sites for catalytic interactions, thus increasing the catalytic activity. Interestingly, we were not able to observe the signal at 154 ppm, assigned to the quaternary carbon atom of the pyridine ring, in the dipolar dephasing spectrum. This would indicate that the pyridine ring is attacked by the oxidative treatment as well. Since no additional confirmation for this statement was conveyed by any other analytical results, it is likely that the polymer decomposition proceeds via backbone cleavage.

In contrast to ^{13}C CP/MAS, solid-state NMR measurements of ^{15}N in natural abundance are still rare, due to the unfavorable NMR properties of this nucleus [17,18]. Nevertheless, a ^{15}N -CP/MAS spectrum of PVP could be obtained. It shows just one resonance at $\delta = -63.2$ ppm in the typical range of pyridines [19]. The ^{15}N CP/MAS spectrum of OsO_4 -loaded PVP (**2a**) is seen in Fig. 3. The signal at $\delta = -64.0$ ppm dominates the spectrum. The $\delta(^{15}\text{N})$ and also the chemical shift anisotropy [13,14] suggest that this signal comes from the support material. Another signal with a very low intensity is also seen. The highest peak has a δ -value of -146 ppm, but this is not necessarily the isotropic line. In order to determine whether this signal

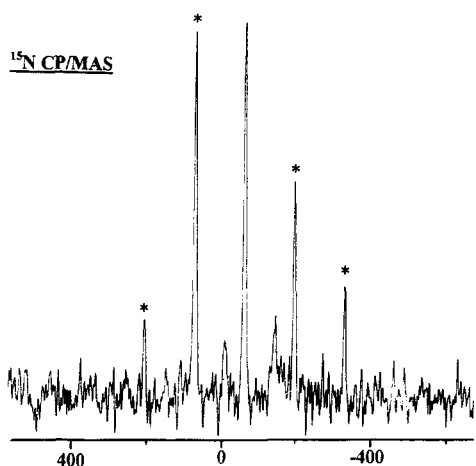


Fig. 3. 30.4 MHz ^{15}N CP/MAS spectrum of poly(4-vinyl pyridine) (PVP) treated with OsO_4 in THF. The asterisks denote rotational sidebands. Spinning frequency: 4060 Hz.

possibly arises from N-atoms bound to osmium, $\text{OsO}_4 \cdot \text{py}$ [20] was used as a model.

Unfortunately, no ^{15}N solid-state NMR signal could be obtained from it, most probably due to the long ^1H relaxation times of > 60 s.

2.3. IR / Raman spectroscopy

Both the IR and Raman spectra have been generated by subtracting the support polymer spectrum from sample spectra. The diffuse reflectance FTIR (DRIFT) spectra of **2a** and **2b** show the following major bands in the spectral range between 600 and 1100 cm^{-1} : **2a** 610 (**2b**: 606), 650 (655), 676 (688), 849 (842), 1040 (1040), and 1060 (1061) cm^{-1} . These signals are well in accord with the photoacoustic FTIR (PA-IR) and Raman measurements (Table 4). Due to the complexation of the OsO_4 there are two different changes in the 'surface' species spectra of **2b**.

The number of bands belonging to the pyridine vibrations at ca. 1065, 1034, 750, and 670 cm^{-1} are shifted as a consequence of the metal-attachment of this molecule. All these bands are active both in the PA-IR and Raman spectra. The second type of new bands belong to Os-oxide species. The clear alternative of the OsO_2 stretching modes, namely the activity of

Table 4

Raman and PA-IR spectra (cm^{-1}) of PVP supported OsO_4 **2b** and PVP supported $\text{K}_2[\text{OsO}_2(\text{OH})_4]$ **2c**; support spectra are subtracted (* positive bands after PVP subtraction)

2b		2c		PVP		Assignments
Raman	infrared	Raman	infrared	Raman	infrared	
1067 s	1065 w	1066 m	1065 m	1071 m	1069 m	py
1031 s	1034 w	1030 m	1033 w	—	—	py-Os
+ 995 vs *	+ 995 w, b *	+ 995 m *	+ 995 vw *	995 vs	994 vs	py
				959 vw		
885 s	890 sh 845 vs	880 s 845 vw	843 vs			OsO_2 sym str. OsO_2 asym str.
				825 sh	825 vs	py
				800 w	800 vw	
745 vw	750 wm,b	747 w	750 vw,b	749 vw	750 m	py
					711 vw	
+ 670 vs *	+ 670 sh *	+ 670 *		669 vs	669 w	py
	651 m		651 s			surface complex
					626 sh	
606 w, b	609 s		607 s, m			surface complex
	550 w,sh		556 w		568 vs	surface complex
470 w	413 m					
					387 w, b	skeletal mode
					220 w	skeletal mode

Table 5
Vibrational frequencies and calculated force constants for O=Os=O grouping in different molecules

	$K_2[\text{OsO}_2(\text{OH})_4]$	$\text{Os}_2\text{O}_6(\text{py})_4$	2b	OsO_4^a
OsO_2 sym. str. (cm^{-1})	844	874	885	965
OsO_2 asym. str. (cm^{-1})	816	842	845	960
K (OsO) (N cm^{-1})	5.99	6.40	6.51	6.79
F (OsO, OsO) (N cm^{-1})	0.20	0.24	0.30	0.67

K: OsO stretching force constant.

F: Stretch–stretch interaction term.

^a OsO_4 has a tetrahedral structure, consequently there is no linear O=Os=O group.

the symmetric O=Os=O stretching mode only in the Raman spectra at 880 cm^{-1} and the appearance of the asymmetric mode at 845 cm^{-1} dominating in the PA-IR, suggests a *linear* O=Os=O grouping. In accord with the DRIFT spectra in the region of Os–O (single bond), stretching bands are found in the PA-IR spectra at 650 and 608 cm^{-1} as bands of medium and strong intensity. The signals can be assigned to Os_2O_2 -stretching modes (B_{2u} and B_{3u}), indicating a *dinuclear* D_{2h} -symmetrical structure. Therefore, we can propose a dinuclear octahedral structure for the surface complex with two *trans*-oriented oxo ligands and bridging oxygen atoms. Furthermore, a weak feature is observed at 550 and 413 cm^{-1} , possibly due to Os–OH stretching modes belonging to a second oxidic Os(VI) structure. Moreover, evidence for the presence of carboxy groups in the polymer after

oxidative treatment is obtained by DRIFT (strong bands for **2b** at 2600 and 1700 cm^{-1}).

Criegee had already described the formation of an osmium(VI) oxide by reduction of OsO_4 with ethanol in the presence of pyridine [20]. The structure was later determined as $\text{Os}_2\text{O}_6(\text{py})_4$ by X-ray crystallography [21]. This compound shows IR signals at 874 cm^{-1} (OsO_2 sym. stretching mode), 842 cm^{-1} (OsO_2 asym. stretching mode), 596 and 643 cm^{-1} (Os_2O_2 stretching modes) [22]. Comparison of the vibrational frequencies and calculated force constants for O=Os=O groupings in different molecules (Table 5) lead to the following conclusions:

(1) Increasing OsO stretching frequencies lead to greater OsO force constants.

(2) The OsO bond strength increases with the oxidation state of the metal.

Table 6
Oxidation of olefins using catalyst **2b** and catalyst **1** in $\text{H}_2\text{O}_2/t\text{-BuOH}$

Starting material	Product	2b (yield (%))	1 (yield (%))
Cyclohexene	1,2-dihydroxy-cyclohexane	76	66
Cyclooctene	1,2-dihydroxy-cyclooctane	99	
Styrene	1,2-dihydroxy-phenylethane	75	0
Cyclooctatetraene	1,2-dihydroxy-3,5,7-cyclooctatriene	45	
1-octene	1,2-dihydroxy-octane	73	33
<i>Trans</i> -4-octene	4,5-dihydroxy-octane	100	
Methyl oleate	methyl 9,10-dihydroxy-undecanoate	92	
Allyl alcohol	glycerol	80	0
1-decene	1,2-dihydroxy-decane	80	31
Ethyl crotonate	ethyl 2,3-dihydroxy-butrate	95	
<i>n</i> -butyl methacrylate	<i>n</i> -butyl 2,3-dihydroxy-2-methyl propionate	100	14
Mesityl oxide	3,4-dihydroxy-4-methyl 2-pentanone	92	0
Methylene cyclobutane	1-hydroxy-1-hydroxy-methyl cyclobutane	100	

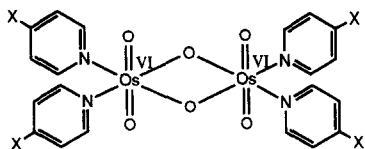


Fig. 4. Structure of oxoosmium(VI)pyridine compounds as models for **2a** and **2b**; X = H, *tert*-butyl, isopropyl.

(3) The close values of the OsO force constants for $\text{Os}_2\text{O}_6(\text{py})_4$ and catalyst **2b** indicate the similarity of the two structures.

In accord with these results, the reaction of OsO_4 and THF in the presence of pyridine and its derivatives leads to similar types of complexes (Fig. 4). Even with the influence of an alkyl group in *para* position (modelling the polymer backbone), the dinuclear Os(VI) structure occurs. These compounds are active as catalysts in the dihydroxylation of alkenes with hydrogen peroxide as the primary oxidant.

The addition of ethanol to OsO_4 and PVP in THF yields **2a** according to IR and XPS. Moreover, the addition of ethanol accelerates the process of reduction and fixation significantly. Following the concept of fully avoiding the extremely poisonous OsO_4 , it is suitable to synthesize a catalytic active sample **2c** by stirring an aqueous solution of potassium osmate with PVP. As compared with **2a** the resulting polymer **2c** shows almost identical spectroscopic data (PA-IR, Raman; Table 4) and similar catalytic activity. Again this method is known for the preparation of $\text{Os}_2\text{O}_6(\text{py})_4$ [23].

The activity of the catalyst **2b** was tested on a wide range of organic substrates. Some of the results are shown in Table 6. Data from the Cainelli-type catalytic system are given for comparison. The results are in line with those reported previously [8]. However, slightly longer reaction times or higher temperatures were occasionally needed. The yields are throughout lower using catalyst **1** under the same catalytic conditions. Under the applied conditions, catalyst **2b** is not active when oxidants other than H_2O_2 were used, e.g. trimethylamine-*N*-oxide, *tert*-butyl hydroperoxide, bis-*tert*-butyl perox-

ide, oxygen, or hexacyanoferrate(III). In case of **1**, however, the best results were obtained by means of trimethylamine-*N*-oxide or *tert*-butyl hydroperoxide [5] — the typical feature of molecular catalysts of types OsO_4 and $\text{OsO}_4 \cdot \text{L}$.

3. Conclusion

Our catalyst system of PVP-grafted osmium oxide proves useful in the catalytic dihydroxylation of olefins by means of hydrogen peroxide. It provides oxidic osmium(VI) in a non-volatile form and is conveniently used for laboratory purposes. The catalyst system can be recycled several times although the polymer support (PVP) is slowly attacked under the oxidative conditions. We are afraid that this gradual polymer decomposition will hamper an industrial application. Nevertheless, there is great potential in polymer-supported OsO_4 catalysts taking into account that — as shown in this paper — reduced species (Os^{VI} , Os^{IV}) are still well-suited as active catalyst precursors.

4. Experimental section

TXRF (total reflection X-ray fluorescence analysis) measurements (Os analysis) were carried out by Professor Schuster and co-workers on a Atomika XSA-8000 in our institute. Elemental analysis (C, H, N), XPS, and DRIFT measurements were performed in the analytical laboratory of the central research department at Hoechst in Frankfurt. Solid-state-NMR: all spectra were recorded on a Bruker MSL 300 and on a Varian VXR 300 NMR spectrometer, equipped with 7 mm double bearing probeheads. The materials were packed densely in 7 mm ZrO_2 rotors and cross polarization (CP) [13,24], dipolar dephasing [13,25], and magic angle spinning (MAS) [13] with rotational speeds of 4 to 4.5 kHz were used. ^{13}C CP/MAS: the recycle delay was 4 s, the contact time 5 ms and for the dipolar dephasing experiments a

delay of 40 μ s was applied. The external reference was adamantane ($\delta = 29.47$ for the low frequency signal [26]), that was also used for the optimization of the Hartmann–Hahn match. About 500 scans gave spectra with satisfactory signal to noise ratio. ^{15}N CP/MAS: recycle delays of 1 to 60 s and contact times of 3 to 8 ms were applied. Depending on the sample numbers of scans ranged between 1000 and 53000. The external reference used was solid $^{15}\text{NH}_4^{15}\text{NO}_3$. The PA-IR spectra were recorded on a Bio-Rad Digilab Division FTS-65A/896 FTIR spectrometer at 4 cm^{-1} optical resolution between 4000 and 400 cm^{-1} using an MTEC 200 photoacoustic detector. The Raman spectra were taken on a Bio-Rad Digilab Division dedicated FT-Raman spectrometer between 3500 and 70 cm^{-1} at 4 cm^{-1} optical resolution employing 40 mW energy of a Nd:YAG excitation laser at the sample position. NMR sample tubes with 5 mm diameter were used as sample holders. The number of accumulated scans were 4096. The spectra were processed employing the GRAMS/386-based WIN-IR software applied with the FT-Raman spectrometer.

Catalysts **1**, **2a** and **2b** [8], and PVP-*N*-oxide [27] were prepared according to literature procedures. Poly(4-vinyl pyridine) (2% cross-linked) and potassium osmate were purchased from Aldrich, OsO_4 from Heraeus. 8% H_2O_2 /*tert*-butanol solutions were used for the oxidation tests and the preparation of **2b**. These solutions were prepared according to the reported method [28]; care was taken to keep the temperature of the mixture at 15–20°C during the H_2O_2 addition.

4.1. Catalyst **2c**

1 g PVP was suspended in a solution of 100 mg potassium osmate in 10 mL H_2O and stirred over night. During the fixation the pink color of the solution disappeared and the color of the polymer turned to brown. The solid was filtered off and dried under reduced pressure.

4.2. A typical oxidation experiment with **2b** as catalyst

25 mg of **2b** (ca. 5% Os) was suspended in 5 to 10 mL H_2O_2 /*tert*-BuOH (8%). Then 0.5 mmol alkene was added at 10–15°C and the reaction mixture was stirred for 4–7 h at room temperature.

4.3. Di- μ -oxo-tetra(oxo)tetrakis(4-*tert*-butyl pyridine)diosmium(VI)

A solution of 270 mg (1.1 mmol) OsO_4 in 2 mL of THF and 1 mL (6.8 mmol) of 4-*tert*-butyl pyridine was allowed to stand for 3–4 days. A brown precipitate or crystals were obtained. The solid was filtered off, washed with *n*-hexane and dried under reduced pressure. Yield: 217 mg (39%), el. anal. found: C 41.7, H 5.5, N 4.9, calc. for $\text{Os}_2\text{O}_6(\text{C}_9\text{H}_{13}\text{N})_4$ (1017.2 g/mol): C 42.5, H 5.5, N 5.2; IR (KBr) ν (cm^{-1}): 570 w, 599 s, 644 s, 837 vs, 1027 m, 1068 m, 1224 m, 1273 m, 1366 m, 1421 s, 1459 m, 1498 m, 1618 s, 2963 s.

Analogous results were obtained with 4-*iso*-propyl pyridine; el. anal. found: C 43.3, H 5.7, N 5.1, calc. for $\text{Os}_2\text{O}_6(\text{C}_8\text{H}_{11}\text{N})_4$ (961.1 g/mol): C 43.0, H 5.8, N 4.6; IR (KBr) ν (cm^{-1}): 580 w, 604 s, 638 m, 840 vs, 1029 m, 1064 m, 1096 m, 1181 m, 1226 w, 1262 m, 1424 s, 1619 s, 2972 s.

Acknowledgements

We thank Dr. O. Althoff and Dipl.-Ing. B. Bock, central research HOECHST AG, for recording the XPS spectra, Dr. M. Kleine/Dipl.-Chem. W. Wachter for recording the TG-MS spectra, and Professor Dr. G. Schuster and co-workers for Os analysis. Furthermore, we thank Professor Dr. R.K. Harris (University of Durham) for fruitful discussions, the Pinguin Foundation for financial support, the Fonds der Chemischen Industrie for a Liebig Fellowship (J.B.), and the Alexander von Hum-

boldt Foundation for a research fellowship (H.B.F.). J.M. thanks the Alexander von Humboldt Foundation for a Senior Scientist Award (1995/96). The FTIR and FT-Raman spectrometer were purchased with the help of the PHARE-ACCORD Programme No. H9112-0152, and the research was supported by a COST D-4 programme. Support came also from the Bayerische Forschungsförderung which is greatly acknowledged at this occasion.

References

- [1] K.A. Hofmann, *Chem. Ber.* 43 (1912) 3329.
- [2] N.A. Milas and S. Sussamman, *J. Am. Chem. Soc.* 58 (1936) 1302.
- [3] R. Criegee, *Justus Liebigs Ann. Chem.* 522 (1936) 75.
- [4] H.C. Kolb, M.S. VanNieuwenhze and K.B. Sharpless, *Chem. Rev.* 94 (1994) 2483.
- [5] G. Cainelli, M. Contento, F. Manescalchi and L. Plessi, *Synthesis* (1989) 45.
- [6] W.R. Griffith and R. Rossetti, *J. Chem. Soc. Dalton Trans.* (1972) 1449.
- [7] B.M. Kim and K.B. Sharpless, *Tetrahedron Lett.* 31 (1990) 3003.
- [8] W.A. Herrmann and G. Weichselbaumer, EP 0 593 425 B1 (1994).
- [9] V.I. Nevedov, *Koord. Khim.* 4 (1978) 1283.
- [10] I.V. Lin'ko, B.E. Zaitsev, A.K. Molodkin, T.M. Ivanova and R.V. Linko, *Russ. J. Inorg. Chem.* 28 (1983) 857.
- [11] B. Folkesson, *Acta Chem. Scand.* 27 (1973) 287.
- [12] J. Blümel, *J. Am. Chem. Soc.* 117 (1995) 2112.
- [13] E.O. Stejskal and J.D. Memory, *High Resolution NMR in the Solid State* (Oxford University Press, New York, 1994), and references therein.
- [14] T.M. Duncan, *A Compilation of Chemical Shift Anisotropies* (The Farragut Press, Chicago, 1990).
- [15] H. Günther, *NMR-Spektroskopie* (Georg Thieme Verlag, Stuttgart, 1992) pp. 478–479.
- [16] H.-O. Kalinowski, S. Berger and S. Braun, ¹³C-NMR-Spektroskopie (Georg Thieme Verlag, Stuttgart, 1984) p. 347.
- [17] R.D. Curtis and R.E. Wasylshen, *Can. J. Chem.* 69 (1991) 834.
- [18] B. Chaloner-Gill, W.B. Euler, P.D. Mumbauer and J.E. Roberts, *J. Am. Chem. Soc.* 113 (1991) 6831.
- [19] J. Mason (Ed.), *Multinuclear NMR* (Plenum Press, New York, 1987).
- [20] R. Criegee, B. Marchand and H. Wannowius, *Justus Liebigs Ann. Chem.* 550 (1942) 99.
- [21] A.M.R. Galas, M.B. Hursthouse, E.J. Behrman, W.R. Midden, G. Green and W.P. Griffith, *Transition Met. Chem.* 6 (1981) 194.
- [22] A.B. Nikol'skii, Y.I. D'yachenko and L.A. Myund, *Russ. J. Inorg. Chem.* 19 (1974) 1368.
- [23] A.M. El-Hendawy, W.P. Griffith, F.I. Taha and M.N. Moussa, *J. Chem. Soc. Dalton Trans.* (1989) 901.
- [24] A. Pines, M.G. Gibby and J.S. Waugh, *J. Chem. Phys.* 59 (1973) 569.
- [25] S.J. Opella and M.H. Frey, *J. Am. Chem. Soc.* 101 (1979) 5854.
- [26] S. Hayashi and K. Hayamizu, *Bull. Chem. Soc. Jpn.* 64 (1991) 685.
- [27] R.J. Forster and J.G. Vos, *Makromolekules* 23 (1990) 4372; D. Böckh, J. Detering and C. Schade, *DE 43 06 606 A 1* (1994).
- [28] N.A. Milas, J.H. Trepagnier, J.T. Nolan and M.I. Iliopoulos, *J. Am. Chem. Soc.* 81 (1959) 4730.